Cell Medicine, Part B of Cell Transplantation, Vol. 1, pp. 105–112, 2010
Printed in the USA.

2155-1790/10 $90.00 + .00
DOI: 10.3727/215517910X451603
www.cognizantcommunication.com

Effects of Quantum Dot Labeling on Endothelial Progenitor Cell Function and Viability

Matyas Molnar,*† Peter Friberg,* Ying Fu,† Mikeal Brisslert,‡ Michael Adams,§ and Yun Chen*†

*Department of Molecular and Clinical Medicine/Clinical Physiology, The Sahlgrenska Academy and University Hospital, University of Gothenburg, Gothenburg, Sweden
†Department of Theoretical Chemistry, School of Biotechnology, Royal Institute of Technology, Stockholm, Sweden
‡Department of Rheumatology and Inflammation Research, The Sahlgrenska Academy and University Hospital, University of Gothenburg, Gothenburg, Sweden
§Department of Pharmacology and Toxicology, Queen's University, Kingston, Ontario, Canada

Endothelial progenitor cells (EPC) play an important role in repairing damaged endothelium. An effective imaging method for in vivo tracking of EPCs is essential for understanding EPC-based cell therapy. Fluorescent quantum dots (QDs) have attractive optical characteristics such as extreme brightness and photostability. QDs are currently being investigated as probes for stem cell labeling; however, there is concern about whether QDs can be used safely. We investigated whether quantum dot (QD) labeling would influence EPC viability and function. Rat bone marrow-derived EPCs were cultured and characterized. The cells were labeled with near-infrared-emitting, carboxyl-coated QDs (8 nM) for 24 h. QD labeling efficiency was higher than 97%. Using WST-1 assay, we showed that the viability of the QD-labeled EPCs was not different from that of the control EPCs. Moreover, QD labeling did not influence the ability of EPCs to form capillary tubes on Matrigel and to migrate. The percentage of QD-positive cells decreased with time, probably due to the rapid division of EPCs. These data suggest that the carboxyl-coated QD705 can be useful for labeling EPCs without interrupting their viability and functions.

Key words: Endothelial progenitor cells; Quantum dots; Cell labeling; Migration; Capillary tube formation

INTRODUCTION

Endothelial progenitor cells (EPC), a subset of bone marrow (BM)-derived progenitor cells, are capable of differentiating into mature endothelial cells (1,14). A low level of circulating EPCs has been shown to be a marker of early phase cardiovascular diseases as a result of risk factors, oxidative stress, nitric oxide activity, or other physiologic processes (4). Although accumulating evidence indicates that progenitor cell therapy has great potential for vascular repair, the regeneration of ischemic tissue, and the promotion of revascularization (5,7,14,17), there is still much debate over the mechanisms of progenitor cell therapy. A noninvasive imaging technique capable of spatially and temporally determining EPC incorporation into vessels in vivo would provide us opportunity to obtain a clear understanding of implanted cell fate.

Different techniques have been used for in vivo tracking of transplanted cells (15). Magnetic resonance imaging (MRI), one of the most commonly used imaging techniques, provides high resolution but has limited sensitivity. Positron emission tomography (PET) and single photon emission computed tomography (SPECT) provide high sensitivity but low resolution and the use of radioactive material limits their biological application. Recently there has been great interest in optical imaging, a very versatile and sensitive imaging tool. Compared with MRI and PET/SPECT, optical imaging is relatively inexpensive without the need of an extensive infrastructure.

One of the newly developed probes used in optical imaging is fluorescent quantum dot (QD) (6,10). Unlike commonly used organic fluorescent dyes, quantum dots (QDs) are semiconductor nanocrystals with attractive optical characteristics such as narrow and symmetric luminescence bands, and high resistance to photobleaching. Due to their extreme brightness and photostability, QDs are ideal for in vivo cell tracking. Near-infrared QDs are of particular interest because tissue autofluores-

Received Feburary 22, 2010; final acceptance October 27, 2010. Online prepub date: November 5, 2010.
Address correspondence to Yun Chen, Associate Professor, Wallenberg Laboratory, Bruna Stråket 16, The Sahlgrenska Academy and University Hospital, University of Gothenburg, SE 413 45 Gothenburg, Sweden. Tel: 46-31-3428407; Fax: 46-31-823762; E-mail: yun.chen@wlab.gu.se

cence is avoided and one can obtain deep tissue imaging (2). Moreover, the narrow emission spectrum and broad excitation spectrum of QDs enable multiple color images to be viewed by single wavelength excitation. Therefore, it is important to investigate whether QDs can be used safely. There is concern about the cytotoxicity of QDs. However, accumulating evidence suggest that this can be minimized by selecting an appropriate shell coating and surface coating, by modulating QD surface charge and/or by using low concentration of QDs (3,12). Most studies relied heavily on the short-term effects of QD labeling on cell viability. Evidence regarding the long-term effects of QD labeling on both cell viability and function is limited.

The aim of this study was to investigate whether QDs can be useful for labeling EPCs without interrupting cell integrity, such as cell viability and their ability to migrate and form capillary tubes. We labeled BM-derived EPCs with near-infrared-emitting, carboxyl-coated QDs, and studied both short-term (immediately after QD exposure) and long-term (several days after QD exposure) effects of QD labeling. Our results showed that the QD-labeled EPCs had normal viability and function, suggesting potential application of QDs for in vivo tracking of EPCs.

MATERIALS AND METHODS

Isolation and Culture of EPCs

For isolating bone marrow cells, tibia and femur bones were removed from male Wistar rats (200–250 g). All experiments were approved by the regional animal ethics committee in Gothenburg, Sweden. After cutting off both ends of the bone shaft, bone marrow was flushed out with prewarmed 2% fetal bovine serum in phosphate-buffered saline (FBS/PBS). Mononuclear cells were separated by density gradient centrifuge (Ficoll-Paque PLUS, GE Healthcare, Sweden) at $400 \times g$ for 25 min at room temperature. The mononuclear cell layer was collected and washed twice with 2% FBS/PBS. The cells were suspended in endothelial growth medium-2 (EGM-2) containing endothelial cell basal medium-2 (EBM-2), SingleQuots (Lonza, Denmark), 20% FBS, 100 U/ml penicillin, 100 μg/ml streptomycin, 29.2 μg/ml glutamine, and 0.25 μg/ml amphotericin B (all from Invitrogen, Sweden), seeded on fibronectin-coated plates (BD Bioscience, Sweden) and incubated at 37°C in a humidified atmosphere with 5% CO_2 in air. After 4-day culture, nonadherent cells were washed away with 2% FBS/PBS. Adherent cells were cultured in EGM-2 with medium replacement every 2–3 days. Colonies of endothelial-like cells were allowed to grow to near confluent, approximately 8–9 days after the isolation.

Characterization of EPCs

To identify EPCs, the adherent cells were incubated with 10 μg/ml 1,1′-dioctadecyl-3,3,′3-tertamethylindocarbocyanine-labeled acetylated low-density lipoprotein (Dil-Ac-LDL, Biomedical Technologies Ltd, UK) at 37°C for 4 h. The labeled cells were visualized with confocal microscopy imaging. Further characterization was performed by staining cells for the expression of endothelial markers CD31, CD34, and Flk1 using immunofluorescence. Briefly, the cells were incubated with primary antibodies against CD31, CD34, and Flk1 (Santa Cruz Biotechnology, USA), respectively. After washing with PBS, the cells were incubated with FITC-labeled anti-rabbit IgG (DakoCytomation, Denmark) or Alexa Fluor 594 anti-mouse IgG (Invitrogen, Sweden). Negative controls were obtained by replacing primary antibodies with 1% BSA. To enable visualization of nuclei, the cells were mounted in Prolong Gold Antifade Reagent with DAPI (Invitrogen, Sweden). Labeling was examined under fluorescence microscopy. From hereafter all cells are determined as EPC.

Quantum Dot Labeling of EPCs

QDs with a CdSeTe core, ZnS shell, and emission maxima at 705 nm (QD705) were purchased from Molecular Probe/Invitrogen (Sweden). In a pilot study, we tested QD705 with two different coatings: carboxyl and PEG-amine. We found that very few cells internalized the PEG-amine-coated QD705, whereas most cells were loaded with carboxyl-coated QD705 after 24-h incubation. In the following studies, only carboxyl-coated QD705 was used. EPCs were detached with 0.05% trypsin/EDTA, suspended in EGM-2 media with or without an addition of 8 nM QD705, and then seeded on different plates. After incubation for 24 h, media were removed and the EPCs (passage 1) were washed three times with PBS. Part of the EPCs was evaluated immediately (e.g., QD labeling efficiency, "short-term" effects of QD labeling on EPC viability and functions), while the rest was kept for "long-term" study of the effects of QD labeling on EPC viability and functions, where the EPCs were cultured up to the third passage. Retention of intracellular QDs was also studied in the EPCs up to the third passage.

Confocal Microscopy

QD labeling efficiency was analyzed visually from a set of confocal images. EPCs were seeded on thin glass slides placed inside a 48-well cell culture plate and cultured in EGM-2 for 24 h. After washing with PBS and fixation using 4% paraformaldehyde for 10 min, the glass slides were rinsed with PBS and mounted using a mounting medium containing DAPI nuclear counter-

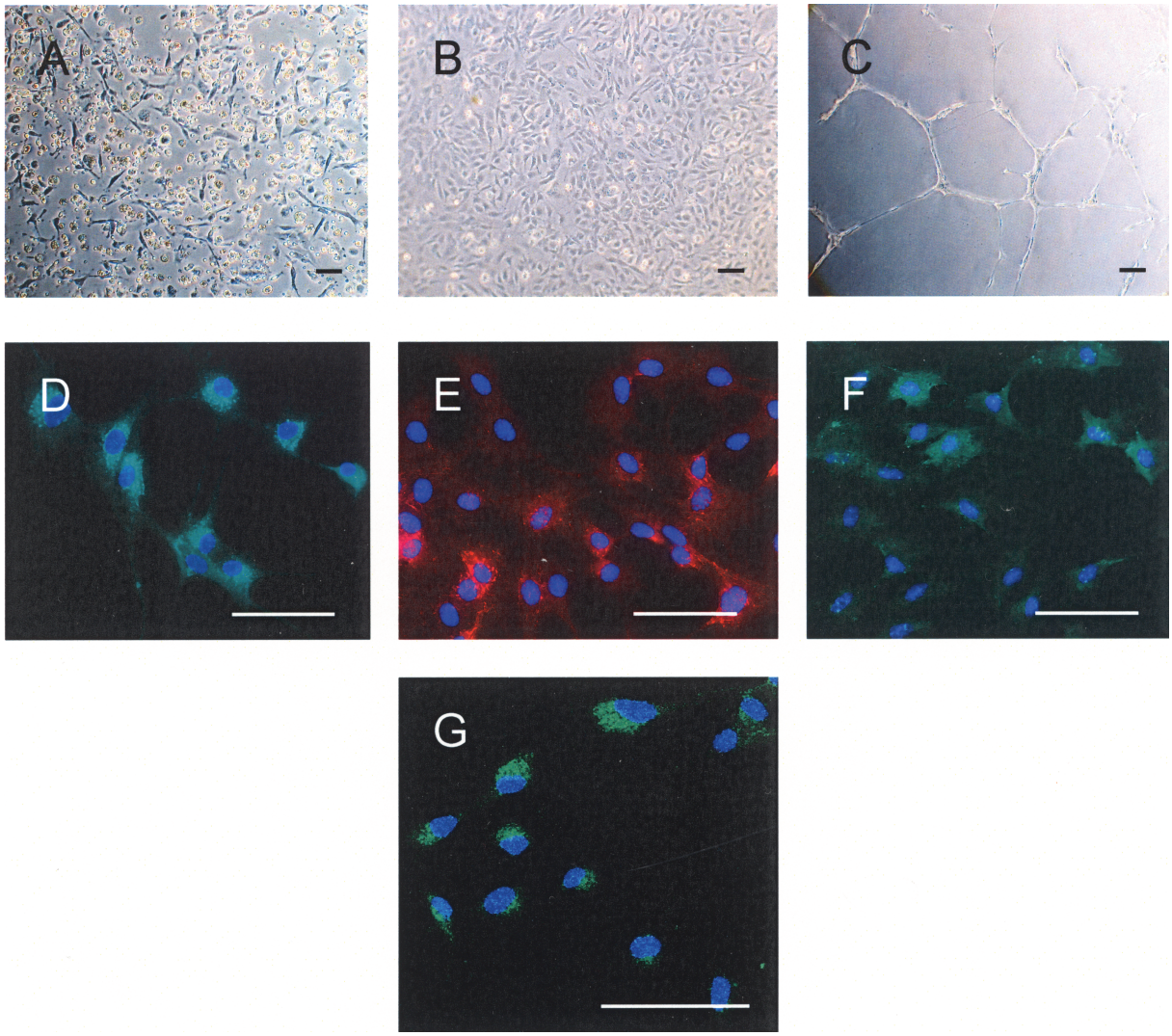

Figure 1. Morphology of bone marrow-derived EPCs on day 4 (A) and day 9 (B) of culture. These cells formed capillary tubes on Matrigel (C), uniformly expressed endothelial cell markers CD31 (D), CD34 (E), Flk-1 (F), and incorporated Dil-Ac-LDL (G). Scale bars: 100 μm.

staining. Intracellular QDs were visualized with Leica TCS SP5 Confocal Microscopy System (excitation at 405 nm and emission at 690–710 nm). About 100–200 EPCs from different images were evaluated and identified as either QD-positive or -negative cells.

Flow Cytometry

QD labeling efficiency was also determined using flow cytometry. EPCs were washed three times with PBS, trypsinized, and resuspended in PBS with 2% fetal bovine serum. Five sets of QD705-labeled EPCs and unlabeled EPCs as control, each containing a minimum of 50,000 viable EPCs, were analyzed using a FACS-Canto II flow cytometer equipped with Diva 6 software (BD Bioscience, Erembodegen, Belgium). Fluorescence was detected using the 488 nm laser and the LP655 nm and LP670 nm filters. Samples were analyzed using the FlowJo software (Tree Star Inc, Ashland, OR, USA).

Transmission Electron Microscopy

Transmission electron microscopy was performed to further determine QD location in EPCs. EPCs were labeled with QDs for 24 h and then fixed in Karnovsky fixative for 2 h, pelleted, and embedded in epoxy resin (Agar 100) for ultramicrotome cut. Sections were examined with a Zeiss 912AB transmission electron microscopy (Carl Zeiss SMT, Oberkochen, Germany). Images were collected with a MegaView III CCD camera

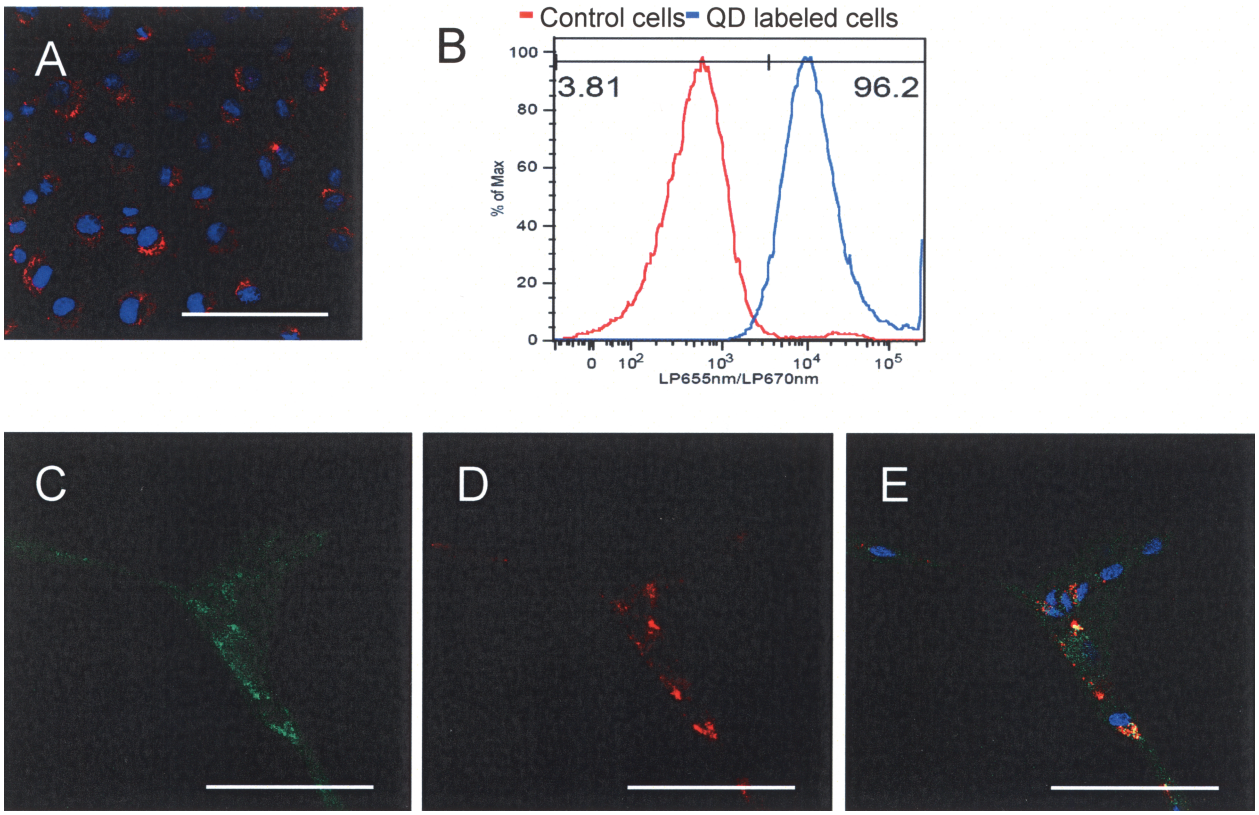

Figure 2. Representative confocal image of EPCs after incubation with 8 nM QDs for 24 h (blue fluorescent is nuclear staining with DAPI; red is QD fluorescence signal). (B) Flow cytometry analysis of QD loading efficiency. (C–E) EPCs that formed capillary tubes are all positive for QDs and took up Dil-Ac-LDL. (C) Dil-Ac-LDL; (D) QD fluorescence; (E) merged image (green: Dil-Ac-LDL; Red: QD fluorescence; blue: nuclear staining with DAPI). Scale bars: 100 µm.

(Olympus/SiS, Münster, Germany) and analyzed with the EsiVision software (Olympus/SiS).

Tube Formation Assay

EPCs (30,000 per well) were plated in a 48-well cell culture plate precoated with 50 µl of Matrigel (BD Bioscience, Sweden) and incubated at 37°C before microscope evaluation of capillary tube formation. Tube formation was quantified by counting the number of tubular structures, which exceed approximately 6 cells in length, in 6 random fields per well after 20 h and 4 days of incubation. Pictures were taken after 4 h of incubation too, but the tube formation was not quantified.

Migration Assay

Migration was examined with a modified Boyden chamber (BD Bioscience, USA). A total of 6×10^5 EPCs suspended in serum-free EBM-2 was placed in the migration chambers and the chambers were immersed in a plate filled with EGM-2 containing vascular endothelial growth factor. After incubation for 20 h, the chambers were washed with PBS and nonmigrated EPC were removed from the upper surface of the membrane with cotton ball. The membrane was fixed with 4% paraformaldehyde for 10 min, stained with hematoxylin, removed, and mounted for evaluation. The number of the migrated cells was quantified by counting EPCs in 6 random high-power fields (400×).

WST-1 Assay

EPCs (10,000 per well) were seeded in a 96-well cell culture plate and cultured for 24 h before 10 µl of WST-1 reagent (Roche, Sweden) was added to each well. After incubation with WST-1 reagent for 4 h at 37°C, the absorbance of the samples was measured at 450 nm.

Statistics

Data are presented as mean ± SD. The statistical significance was determined with Student's *t*-test. A value of $p \leq 0.05$ was considered statistically significant.

RESULTS

Bone Marrow Monocyte-Derived EPCs

To obtain EPCs, bone marrow-derived monocytes were cultured on fibronectin-coated dish. After 4 days in culture, adhered cells appeared as colonies of spindle-shaped cells (Fig. 1A). After 9 days in culture, endothelial cell-like cobblestone morphology was observed (Fig. 1B). These cells formed capillary tubes when reseeded onto Matrigel, expressed endothelial cell markers CD31, CD34, and Flk-1, and incorporated Dil-Ac-LDL (Fig. 1C–G). These data confirmed that the bone marrow-derived cells have endothelial phenotype after 9 days of culture. We thus refer to these cells as EPCs.

QD Labeling of EPCs

To label EPCs, we incubated cells with 8 nM QD705 for 24 h. We observed cytoplasmic distribution of QD705 in the EPCs (Fig. 2A). Visual analysis showed that virtually all EPCs were loaded with QDs (99.6 ± 1.1%). This was confirmed by flow cytometry (97.2 ±

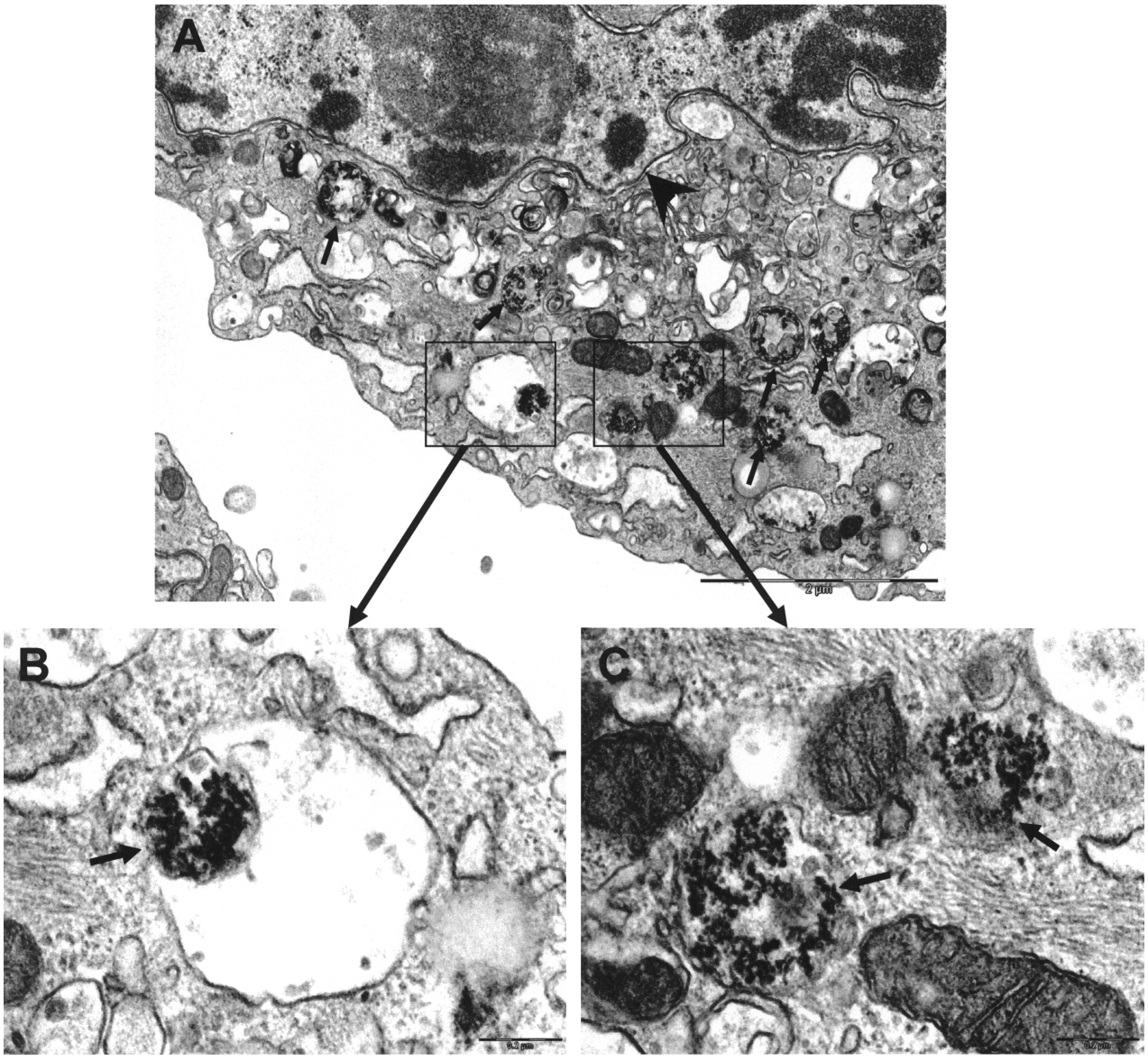

Figure 3. TEM of QD-labeled EPCs. (A) Low magnification, representative image of EPC with QD nanocrystals in endosomal/lysosomal vesicles (arrows). Arrowhead denotes nuclear membrane. Scale bar: 2 μm. (B, C) High magnification of vesicles showing individual QDs. Scale bars: 200 nm.

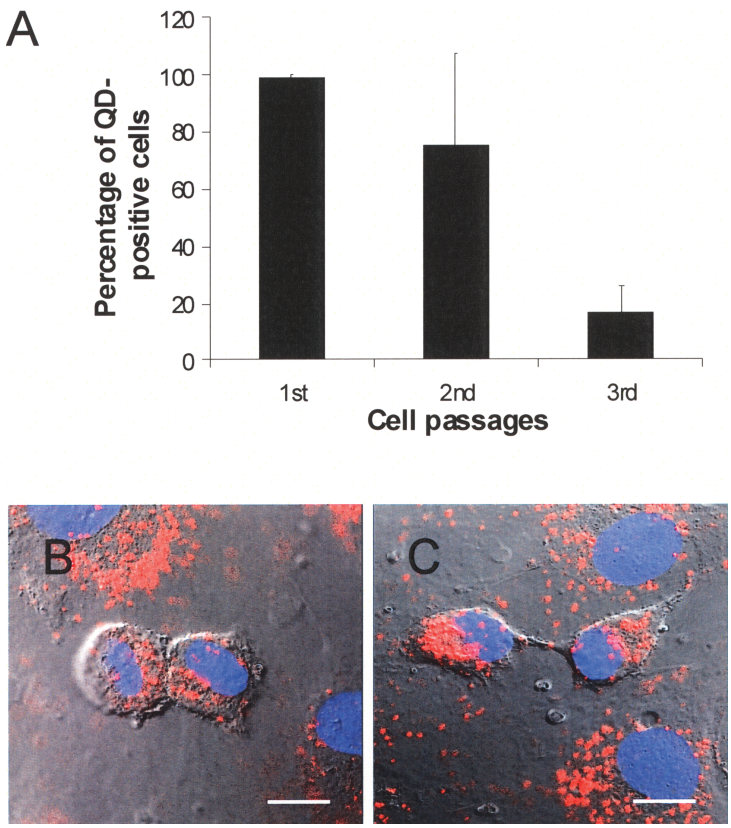

Figure 4. (A) Percentage of QD-positive EPCs at passage 1, 2, and 3, expressed as mean ± SD ($n = 8$). (B, C) QDs are divided into two daughter cells. Red: QD fluorescence; Blue: nuclear staining with DAPI. Scale bars: 10 μm.

1.3% of 50,000 cells analyzed, $n = 5$) (Fig. 2B). Moreover, cells that formed capillary tubes were all positive for QDs and incorporated Dil-Ac-LDL (Fig. 2C–E). TEM images of QD-labeled EPCs showed that there were many QD nanocrystals in endosomal/lysosomal vesicles (Fig. 3), indicating that QD labeling was effective.

Although QDs remained visible inside the EPCs at day 4–5 (passage 2) and day 7–10 (passage 3) after the initial QD exposure, the percentage of QD-positive cells decreased with time (Fig. 4A). Furthermore, we observed that QDs were asymmetrically divided into two daughter cells (Fig. 4B, 4C).

Effects of QD Labeling on EPC Viability and Function

To determine the effect of intracellular QDs on cell viability and function, we cultured QD-labeled EPCs for three passages. Using WST-1 assay, we showed that the viability of the QD-labeled EPCs was not different from that of the control EPCs (100.6 ± 7.7%, 98.6 ± 7.8%, and 97.6 ± 3.7% of the controls for passage 1, 2, and 3, respectively). We also performed tube formation assay and migration assay to evaluate whether QD loading might influence the ability of EPCs to form capillary tubes and to migrate. We did not observe any difference between QD-loaded EPCs and control EPCs in tube formation (Fig. 5) and migration potential (Fig. 6).

DISCUSSION

EPC-based cell therapy holds great potential for treatment of cardiovascular diseases (5,14). Understanding the mechanisms underlying the EPC-based cell therapy requires effective imaging methods for in vivo tracking of EPCs. In the present study we cultivated and characterized bone marrow-derived EPCs. Our data established that the QD705-labeled EPCs had normal viability and maintained normal ability to migrate and form capillary tubes, suggesting potential application of QD705 for in vivo tracking of EPCs.

QDs are increasingly being used for tracking stem cells (8,11,13,16). An ideal labeling technique should be efficient and easy to apply, while contrast agents should be nontoxic for cells and not interfere with cell function. Emerging data suggest that the cytotoxicity of QDs can be minimized by selecting an appropriate shell and surface coating, by modulating QD surface charge, and/or

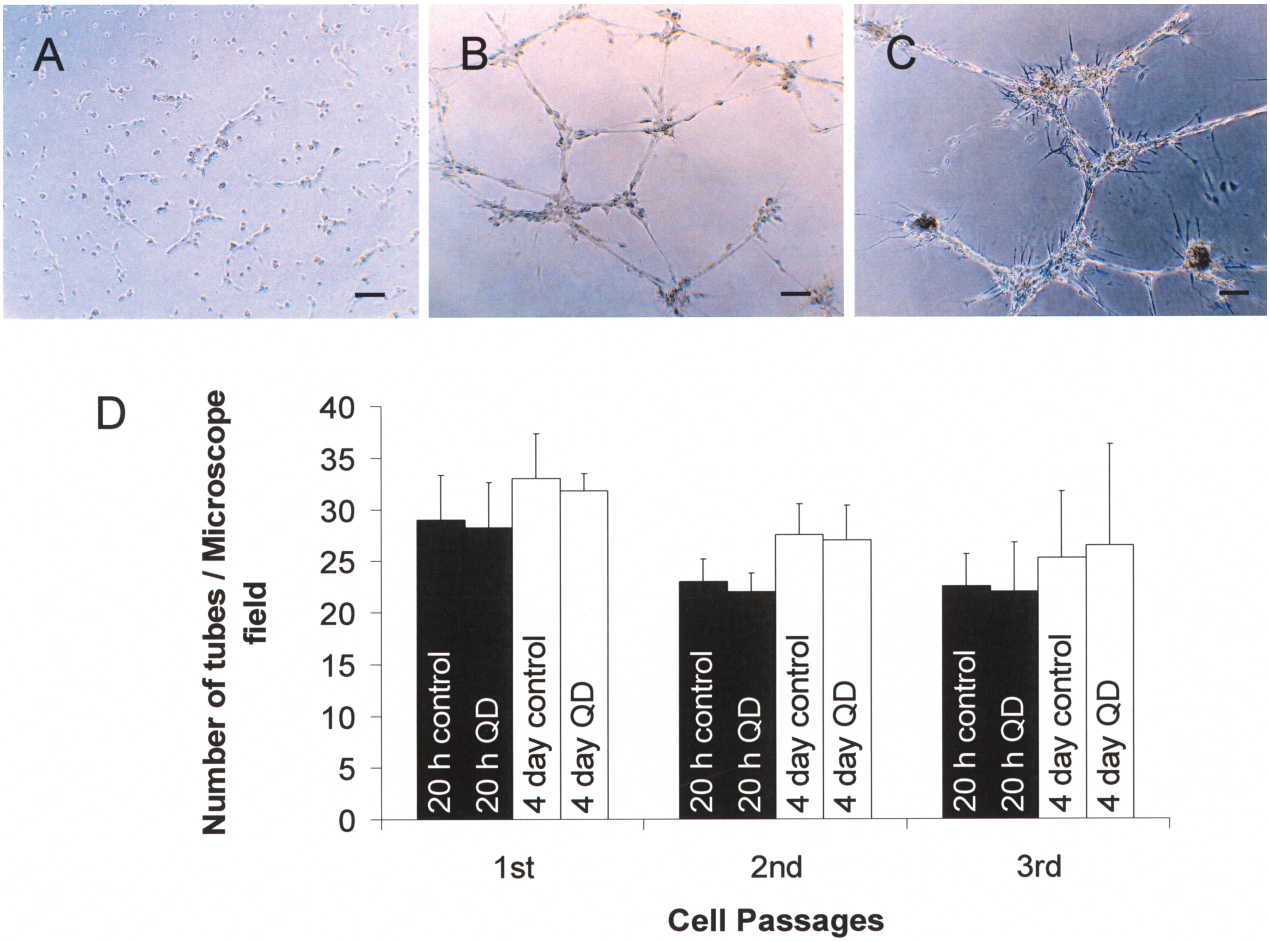

Figure 5. Tube formations of EPCs after 4 h (A), 20 h (B), and 4 days (C) of incubation on Matrigel. Scale bars: 100 µm. (D) Quantitative tube number per microscopic field, expressed as mean ± SD ($n = 4$).

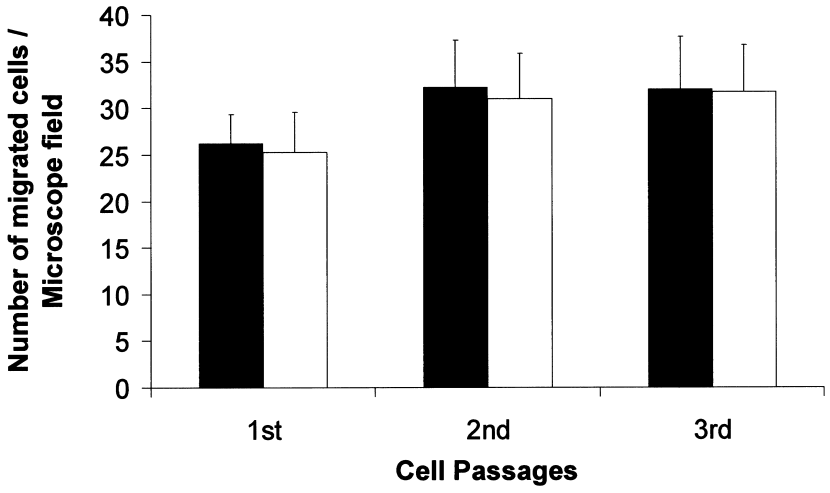

Figure 6. Number of migrated cells per microscope field, expressed as mean ± SD ($n = 4$). The migration ability of the QD-labeled EPCs (white bars) did not differ from that of the control EPCs (black bars).

by using low concentration of QDs (3,12). In this study, we used negatively charged carboxyl-coated QDs. We found that the EPCs can be labeled efficiently by incubating with 8 nM of carboxyl-coated QD705 for 24 h. We evaluated both short-term (immediately after QD exposure) and long-term (several days after QD exposure) effects of QD labeling. Our data showed that the QD labeling did not change EPC morphology or metabolic activity. Moreover, the essential EPC functions such as migration and tube formation were not affected by the QD labeling. It has been shown that carboxyl-coated QDs are recognized by lipid rafts in human epidermal keratinocytes and internalized into the endosomes/lysosomes (18). Subcellular distribution of QDs is known to be affected by QD size (9). Interestingly, larger QDs (5.2 nm) located in the cytoplasm are apparently less cytotoxic than smaller QDs (2.2 nm) distributed in the nucleus (9). We found that the QD705 were located in the cytoplasm, but not the nucleus, of the EPCs, probably due to the large size of QD705 (18.5 nm). Thus, the low concentration (8 nM), negative surface charge, and large size may have contributed to the fact that the carboxyl-coated QD705 can be used safely for labeling EPCs.

We have followed the QD-labeled EPCs for up to the third passage. Although QDs remained visible in the EPCs of the third passage, the percentage of the QD-positive EPCs dropped to 20%. This dramatic decrease could be due to the rapid division of EPCs. We found that QDs actually divided into daughter cells, which could lead to a dilution of QDs reaching levels below detection limits. Moreover, QDs may be divided asymmetrically into daughter cells, which resulted in fewer cells remaining QD labeled at the third passage. The short retention of QDs in cells suggests that QD-labeled EPCs are more suitable for studying EPC engraft and differentiation in the host environment while cells still remain their cellular labeling rather than for long-term tracking.

In summary, the carboxyl-coated QD705 can be useful for labeling EPCs without interrupting their viability and functions. The QD labeling method that we present here is apparently efficient (almost all cells were labeled) and easy adaptable technique (no special transfection agent needed) in living cells.

ACKNOWLEDGMENTS: This study was supported by VINNOVA (Project number P35914-1), Sahlgrenska University hospital funds (ALF-support) and Wilhelm & Martina Lundgren Foundation.

REFERENCES

1. Asahara, T.; Murohara, T.; Sullivan, A.; Silver, M.; van der Zee, R.; Li, T.; Witzenbichler, B.; Schatteman, G.; Isner, J. M. Isolation of putative progenitor endothelial cells for angiogenesis. Science 275(5302):964–967; 1997.
2. Aswathy, R. G.; Yoshida, Y.; Maekawa, T.; Kumar, D. S. Near-infrared quantum dots for deep tissue imaging. Anal. Bioanal. Chem. 397(4):1417–1435; 2010.
3. Hardman, R. A toxicologic review of quantum dots: Toxicity depends on physicochemical and environmental factors. Environ. Health Perspect. 114(2):165–172; 2006.
4. Hill, J. M.; Zalos, G.; Halcox, J. P.; Schenke, W. H.; Waclawiw, M. A.; Quyyumi, A. A.; Finkel, T. Circulating endothelial progenitor cells, vascular function, and cardiovascular risk. N. Engl. J. Med. 348(7):593–600; 2003.
5. Hung, H. S.; Shyu, W. C.; Tsai, C. H.; Hsu, S. H.; Lin, S. Z. Transplantation of endothelial progenitor cells as therapeutics for cardiovascular diseases. Cell Transplant. 18(9):1003–1012; 2009.
6. Jayagopal, A.; Russ, P. K.; Haselton, F. R. Surface engineering of quantum dots for in vivo vascular imaging. Bioconjug. Chem. 18(5):1424–1433; 2007.
7. Leone, A. M.; Valgimigli, M.; Giannico, M. B.; Zaccone, V.; Perfetti, M.; D'Amario, D.; Rebuzzi, A. G.; Crea, F. From bone marrow to the arterial wall: The ongoing tale of endothelial progenitor cells. Eur. Heart J. 30(8):890–899; 2009.
8. Lin, S.; Xie, X.; Patel, M. R.; Yang, Y. H.; Li, Z.; Cao, F.; Gheysens, O.; Zhang, Y.; Gambhir, S. S.; Rao, J. H.; Wu, J. C. Quantum dot imaging for embryonic stem cells. BMC Biotechnol. 7:67; 2007.
9. Lovric, J.; Bazzi, H. S.; Cuie, Y.; Fortin, G. R.; Winnik, F. M.; Maysinger, D. Differences in subcellular distribution and toxicity of green and red emitting CdTe quantum dots. J. Mol. Med. 83(5):377–385; 2005.
10. Michalet, X.; Pinaud, F. F.; Bentolila, L. A.; Tsay, J. M.; Doose, S.; Li, J. J.; Sundaresan, G.; Wu, A. M.; Gambhir, S. S.; Weiss, S. Quantum dots for live cells, in vivo imaging, and diagnostics. Science 307(5709):538–544; 2005.
11. Molnar, M.; Fu, Y.; Friberg, P.; Chen, Y. Optical characterization of colloidal CdSe quantum dots in endothelial progenitor cells. J. Nanobiotechnol. 8(1):2; 2010.
12. Pelley, J. L.; Daar, A. S.; Saner, M. A. State of academic knowledge on toxicity and biological fate of quantum dots. Toxicol. Sci. 112(2):276–296; 2009.
13. Slotkin, J. R.; Chakrabarti, L.; Dai, H. N.; Carney, R. S.; Hirata, T.; Bregman, B. S.; Gallicano, G. I.; Corbin, J. G.; Haydar, T. F. In vivo quantum dot labeling of mammalian stem and progenitor cells. Dev. Dyn. 236(12):3393–3401; 2007.
14. Steinmetz, M.; Nickenig, G.; Werner, N. Endothelial-regenerating cells: An expanding universe. Hypertension 55(3):593–599; 2010.
15. Villa, C.; Erratico, S.; Razini, P.; Fiori, F.; Rustichelli, F.; Torrente, Y.; Belicchi, M. Stem cell tracking by nanotechnologies. Int. J. Mol. Sci. 11(3):1070–1081; 2010.
16. Yukawa, H.; Mizufune, S.; Mamori, C.; Kagami, Y.; Oishi, K.; Kaji, N.; Okamoto, Y.; Takeshi, M.; Noguchi, H.; Baba, Y.; Hamaguchi, M.; Hamajima, N.; Hayashi, S. Quantum dots for labeling adipose tissue-derived stem cells. Cell Transplant. 18(5):591–599; 2009.
17. Zampetaki, A.; Kirton, J. P.; Xu, Q. Vascular repair by endothelial progenitor cells. Cardiovasc. Res. 78(3):413–421; 2008.
18. Zhang, L. W.; Monteiro-Riviere, N. A. Mechanisms of quantum dot nanoparticle cellular uptake. Toxicol. Sci. 110(1):138–155; 2009.